Physical Modeling of MEMS Cantilever Beams and the Measurement of Stiction Force

Tai Lam and Robert B. Darling

Dept. of Electrical Engineering, Box 352500
University of Washington, Seattle, WA, USA
tailam@ee.washington.edu

ABSTRACT

A finite element model is combined with experimental data to extract the stiction force in MEMS cantilever beams. The model predicts cantilever behaviors both before and after snap-down has occurred. Experimental measurements of cantilevers have been performed to validate the model. With a reliable model and additional experimental data the stiction force between surfaces of MEMS devices can be extracted to predict device behavior or for process control.

Keywords: stiction, cantilever beams, finite element method.

INTRODUCTION

Stiction force is one of the dominant forces that govern MEMS devices, yet it is the least understood and difficult to quantify [1]. Earlier works have used the minimum energy method and analytical approximations to calculate the stiction force [2,3]. The adhesion parameter is given in units of energy per unit area, which is not readily useful in predicting device behavior where knowledge of force per unit area is more important. A conversion between force and energy is not possible in most cases because the stiction mechanisms are not known in an uncontrolled environment. This paper presents a method that combines accurate finite element modeling and experimental measurements of MEMS cantilever beams to quantitatively extract the stiction force [4]. A systematic method to measure stiction force is required for predicting MEMS device behavior as well as for process control.

The typical geometry of a cantilever beam is illustrated in Figure 1. A finite element model of the beam is implemented to include both small and large deflections (cases 1 and 2 in Fig.1). Due to the highly nonlinear nature of electrostatic actuation, a quasi-static, iterative approach is used to insure convergence. For Case 1, a constant deflection profile is assumed at first. Electrostatic loading is calculated and a new deflection profile is determined via the differential equations. The process is iterated until convergence or snap-down occurs. For Case 2, a binary search is combined with iteration to determine the beam profile, which is characterized primarily by the last contact point with the dielectric layer at L'.

Due to stiction force, beams longer than a certain length do not snap back up once snap-down has occurred and the bias-voltage has been reset to zero. The contact area with the dielectric layer has been measured using an optical microscope. From the mathematical model the voltage that produces an equivalent contact area is determined.

From this corresponding voltage, the electrostatic attractive force can be calculated for the area touching the dielectric layer. The stiction force is approximately equal to the calculated electrostatic force since the electrostatic inverse square law implies that most of the attractive force arises from the contacting area.

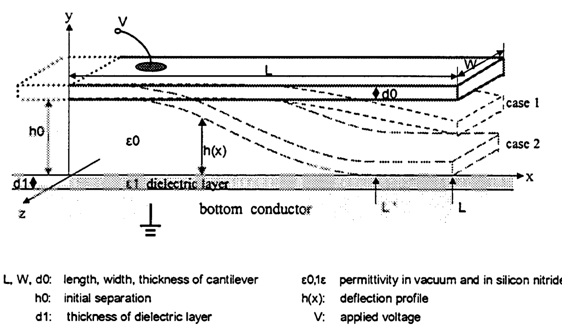

Figure 1. Typical geometry of a cantilever beam.

NUMERICAL METHODS

The governing equation for an Euler-Bernoulli beam undergoing small deflection is

$$EI\frac{d^4 v(x)}{dx^4} = -q(x)\,, \tag{1}$$

where E is Young's Modulus, $I = \frac{W d_0^{\;3}}{12}$ is the cross-sectional area moment of inertia, and $v(x)$ is the deflection profile from equilibrium due to loading $q(x)$. The large ratio of length L over initial gap distance h_0 in the experimental samples meets the small deflection criteria of Euler-Bernoulli beams, even when the tip first touches down.

The electrostatic loading per unit length $q(x)$ is given by the attractive force between two capacitor plates

$$q(x) = -\frac{\varepsilon V^2 W}{2[h(x)]^2}\left(1 + \frac{0.65 h(x)}{W}\right) \quad , \tag{2}$$

where V is the bias voltage between the cantilever and the ground plane, and $h(x)$ is the height of the cantilever above the ground plane. The first term is the familiar capacitor parallel plate attraction force. The second term on the right is to compensate for fringing-field effects. $h(x)$ is the unknown profile, and is given by

$$h(x) = h_0 + v(x)\,. \tag{3}$$

Since the beam bends downward, $v(x)$ is negative. Combining (1)-(3) produces the governing differential equation for cantilever beams under electrostatic attraction

$$EI\frac{d^4 v(x)}{dx^4} = \frac{1}{2}V^2 W \frac{\left(1 + \frac{0.65\left(h_0 + v(x)\right)}{W}\right)}{\varepsilon_0\left(\frac{d_1}{\varepsilon_1} + \frac{h_0 + v(x)}{\varepsilon_0}\right)^2}\,. \tag{4}$$

Equation (4) is highly nonlinear due to the fact that the electrostatic force is inversely proportional to the square of the separation. To solve for the profile $h(x)$ an iterative, quasi-static approach is used [4,5]. First the initial gap is used to calculate uniform loading for the whole beam, for a given bias voltage V. From this loading a beam profile is calculated. The new beam profile, now a function of x, is then used to recalculate the loading. The process is repeated until convergence takes place, i.e. when two successive iterations give nearly identical profiles. Convergence takes place at the equilibrium profile when the electrostatic force balances the mechanical restoring force of the beam. If a bias voltage greater than the snap-down voltage of the beam is used, the beam profile will bend downward until stopped by the ground plane.

The iterative approach is implemented using the finite element method. The beam is first discretized into individual beam elements connected by nodes. The stiffness matrices of each element are calculated and assembled to form the global stiffness matrix. This is put into the familiar form of Hooke's law

$$KD = F\text{ , or } D = K^{-1}F\,, \tag{5}$$

where K is the global stiffness matrix, D is the nodal displacement vector , and F is the nodal force vector. Once the displacement vector D is computed, a new beam profile is determined and a new force vector is calculated. The process is iterated until a convergent profile is found. At each iteration step appropriate boundary conditions are applied using the matrix partitioning method [6].

Figure 2 illustrates the fast convergence of the iteration process for case 1. Even at a bias voltage near the snap-down voltage (2.35 Volts), convergence is reached after only a few iterations.

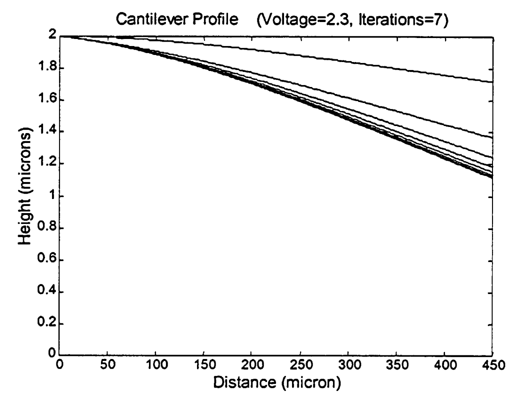

Figure 2. Cantilever profiles for successive iterations before snap-down has occurred (case 1).

After snap-down has occurred the parameter of interest is the percentage of the beam in contact with the dielectric layer, specifically the location of the last contact point between the two surfaces. Binary search is combined with iteration to achieve this. First, for a given bias voltage V, an arbitrary last contact point is assumed. Iteration is then used to determine the profile of the non-contacting part of the beam. If this profile mathematically protrudes into the dielectric layer, the remaining part is too "soft" for the given voltage so the contact point is moved to the left. Similarly if the convergent profile does not protrude into the dielectric layer, it is considered too "stiff" so the contact point is moved to the right. The binary search quickly pinpoints the correct location of the last contact point. Figure 3 illustrates the convergent profile after several iterations and binary searches. A straight line has been used as the initial guess profile. The profile takes up its characteristic shape after only one iteration and converges only a few iterations after that.

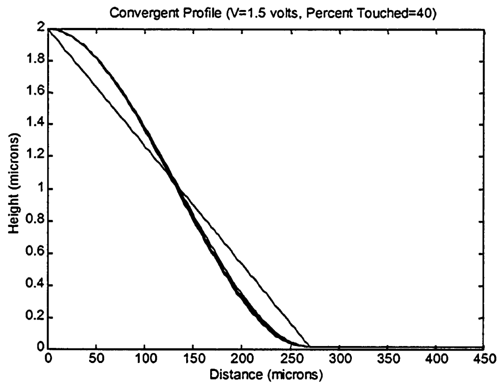

Figure 3. Cantilever profiles for successive iterations after snap-down has occurred (case 2).

EXPERIMENTAL VALIDATION

Before a model could be used with any confidence, experimental data is necessary to validate it. Cantilevers fabricated using MCNC/CRONOS MUMPS process [7] were measured to compare with the model. Figure 4 shows a test chip containing an array of cantilevers used in the measurements. The cantilever width is 10 microns and lengths range from 200 to 550 microns. They are made using the Poly1 layer in MUMPS and are 2 microns thick. The ground plane is the Poly0 layer, which gives a height of 2 microns at the supporting point. A thermal oxide layer 10 nm thick is assumed to coat all Poly surfaces, so the dielectric layer separating the cantilevers and the ground plane is nominally 20 nm.

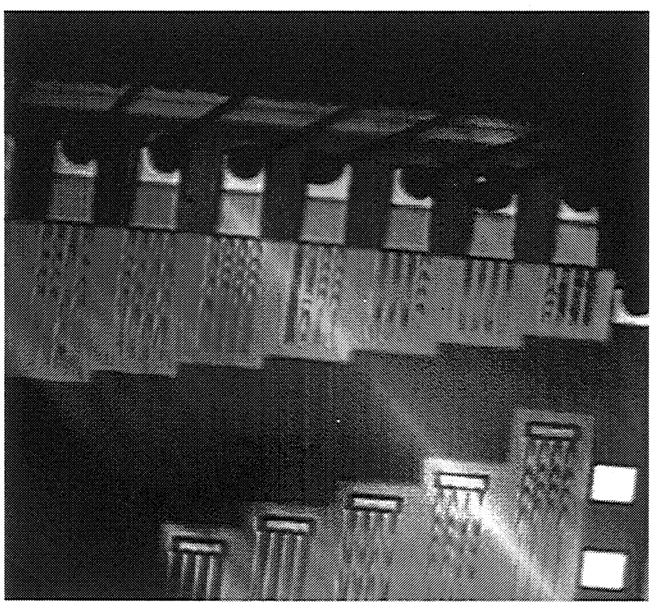

Figure 4. An array of cantilevers of various lengths used in the measurements.

Two cantilever parameters easily measured are the snap-down voltage in case 1 and the percent of beam touching the dielectric layer in case 2; hence, they are the parameters used for comparison.

An optical microscope probe station was used to observe the cantilever behavior. The optical microscope could be viewed through an eyepiece or a CCD camera output on a TV monitor. As the bias voltage is increased the cantilever movements can easily be detected by changes in the fringe and contrast pattern. The bias voltage is slowly increased until a sudden change in fringe pattern indicates that snap-down has occurred.

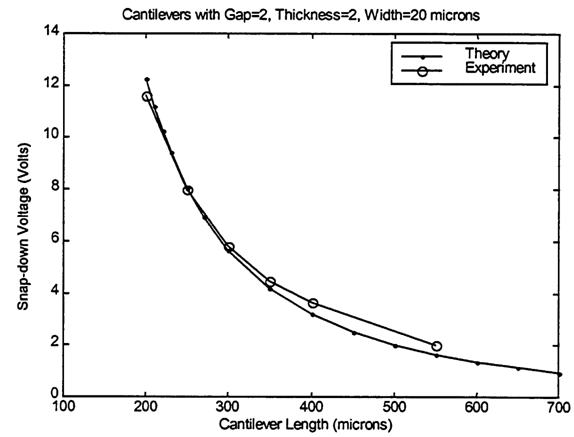

Figure 5. Comparison of measurements versus theory for the snap-down voltage (case 1).

The measured snap-down voltages for cantilevers of different lengths are compared to the model predictions in Figure 5. The agreement is quite good considering that visual detection had been used.

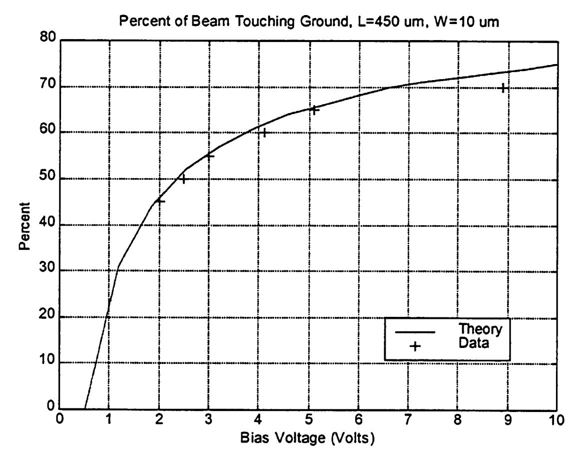

Figure 6. Comparison of measurements versus theory for the percentage of beam touching the dielectric layer (case 2).

After snap-down has occurred the bias voltage is again slowly increased. More of the beam touches the dielectric and the contact point rolls towards the support post. The percentage of beam that touches the dielectric was measured for various bias voltages and compared to the model. Figure 6 shows good agreement between theory versus measurement data.

Good agreement between the model and measurement data suggests that the model is reliable and can be used to extract the stiction force.

CALCULATION OF STICTION FORCE

From experimental observation cantilevers longer than a certain length do not snap back up once snap-down has occurred and the bias voltage is reset to zero. These longer cantilevers have weaker mechanical restoring force and larger contact area so stiction force pins them down.

The contact area with the dielectric layer is measured experimentally. The mathematical model is then used to find a bias voltage that would result in an equivalent contact area. For example, from Figure 6, if the contact area is measured to be 50 percent of the whole beam then the voltage required to achieve this, if stiction force was not present, would be 2.3 Volts. From this corresponding voltage, the electrostatic attractive force can be calculated for the part touching the dielectric layer using Eq. (2). The stiction force is approximately equal to the calculated force since most of the attractive force arises from the area touching the dielectric layer. Note that the stiction force values are highly dependent on the wet release processes, surface roughness, and operating environment.

Beams of different lengths need to be measured so the data analysis can account for the fact that in very long cantilevers the stiction force is active in only a certain fraction of the contact area. The rest of the contact area closer to the tip just sits idle and does not contribute to the pin-down of the cantilever.

Table 1. Experimental data for beams of various lengths.

Length (μm)	% Touching Ground	Equivalent Voltage (V)	Stiction (kPa)
250	10	2.3	228
450	50	2.3	228
500	55	2.5	270

Table 1 shows measurement results for three different beam lengths. The idling effect of longer beams begins to show up in the 500-micron beam and gives an over-estimate of the stiction force. The stiction force between the Poly0 and Poly1 layer of the MUMPS process is determined to be about 228 kPa, a little over twice the atmospheric pressure. Further measurements using a more accurate method [8] inside a vacuum chamber are necessary to ensure that the value is accurate and not affected by atmospheric ambient pressure. This method for measuring the contact stiction force can be extended to other processes and structures.

SUMMARY

A finite element model of a cantilever beam has been developed to include both the before snap-down and after snap-down cases. Iteration and binary search are used to determine the cantilever profile under electrostatic attraction due to a bias voltage. The model is validated by experimental measurements using an optical microscope. The snap-down voltage in case 1 and contact area in case 2 are the comparison parameters.

With a reliable model, additional data has been taken to extract the contact stiction force. For the Poly0 and Poly1 layers of the MUMPS process, the stiction force is determined to be 228 kPa.

REFERENCES

[1] N.R. Tas, et al, "Stiction in Surface Micromachining," J. Micromech. Microeng., vol. 6, 1996, pp. 385-397.
[2] N.R. Tas, et al, "Static Friction in Elastic Adhesive MEMS Contacts, Models and Experiments,", JMSM, vol. 7, no. 3, 1998, pp. 193-198.
[3] C.H. Mastrangelo and C.H. Hsu, "A Simple Experimental Technique for the Measurement of the Work Adhesion of Microstructures," Proc. IEEE Solid-State Sensors and Actuators Workshop, Hilton Head, SC, 1992, pp. 208-212.
[4] T. Lam "Physical Modeling and Experimental Validation of MicroElectroMechanical (MEMS) Beams," Master's Thesis, University of Washington, 2000.
[5] T. Lam and R.B. Darling "Modeling of Focused Ion Beam Trimming of Cantilever Beams" *Proc. 2000 Int. Conf. on Modeling and Simulation of Microsystems (MSM 2000)*, San Diego, CA, USA, pp. 79-82, Computational Publications, 2000.
[6] S.M. Lepi, *Practical Guide to Finite Elements: A Solid Mechanics Approach*. New York: Marcel Dekker, Inc., 1998.
[7] CRONOS Integrated Microsystems, Inc. http://www.memsrus.com/cronos/svcsmumps.html
[8] B. Jensen, et al, "IMAP: Interferometry for Material Property Measurement in MEMS", *Proc. 1999 MSM Conf.*, pp. 206-209, San Juan, Puerto Rico, Apr. 19-21, 1999.